Phase Transitions in Electron Spin Resonance Under Continuous Microwave Driving

A. Karabanov, D. C. Rose, W. Köckenberger, J. P. Garrahan, and I. Lesanovsky
School of Physics and Astronomy, University of Nottingham, University Park, Nottingham NG7 2RD, United Kingdom and Centre for the Mathematics and Theoretical Physics of Quantum Non-equilibrium Systems, University of Nottingham, Nottingham NG7 2RD, United Kingdom

(Received 5 April 2017; published 11 October 2017)

We study an ensemble of strongly coupled electrons under continuous microwave irradiation interacting with a dissipative environment, a problem of relevance to the creation of highly polarized nonequilibrium states in nuclear magnetic resonance. We analyze the stationary states of the dynamics, described within a Lindblad master equation framework, at the mean-field approximation level. This approach allows us to identify steady-state phase transitions between phases of high and low polarization controlled by the distribution of disordered electronic interactions. We compare the mean-field predictions to numerically exact simulations of small systems and find good agreement. Our study highlights the possibility of observing collective phenomena, such as metastable states, phase transitions, and critical behavior, in appropriately designed paramagnetic systems. These phenomena occur in a low-temperature regime which is not theoretically tractable by conventional methods, e.g., the spin-temperature approach.

DOI: 10.1103/PhysRevLett.119.150402

Introduction.—The control and detection of magnetization arising from a polarized ensemble of unpaired electron spins forms the basis of electron spin, or paramagnetic, resonance (EPR), a powerful spectroscopy tool for studying paramagnetic materials placed in a static external magnetic field. The underpinning key principle for this technique is the application of oscillating magnetic fields close to or at the electronic Larmor frequency (usually in the microwave regime) to generate nonequilibrium distributions of populations and coherences between quantum states that lead to detectable signals [1–3]. The evolution of systems of isolated or only weakly coupled paramagnetic centers under the effect of these fields is well understood. A more challenging problem is to predict the response of strongly coupled electron ensembles to such perturbations, particularly in samples in the solid state in which anisotropic components of the electronic interactions are not averaged out by thermal motion. Insight into the dynamics of strongly coupled, microwave-driven electronic ensembles is also needed in order to improve our understanding of dynamic nuclear polarization (DNP), which is an out-of-equilibrium technique to enhance the sensitivity of nuclear magnetic resonance (NMR) applications by orders of magnitude (see, e.g., Ref. [4–6]); in particular, this concerns the cross effect and thermal mixing DNP mechanisms [7–13].

Here we shed light on the nonequilibrium stationary states of a strongly interacting electronic ensemble under continuous microwave driving and subject to dissipation to the environment. We model the dynamics of this system in terms of a Markovian master equation and use a mean-field approximation to compute the steady-state phase diagram. This reveals phase transitions between states of high and low electronic polarization as well as the emergence of a critical point that displays Ising universality [14]. These features are controlled by the distribution of the disordered electronic spin-spin interactions. The uncovered mean-field transitions imply the emergence of metastable states and accompanying intermittent dynamics [15–17], which we confirm numerically through simulations of small systems. Our results suggest that under appropriate conditions collective phenomena such as metastability, phase transitions, and critical behavior should be observable in driven-dissipative, paramagnetic systems. These predictions complement those of conventional theoretical approaches, based, e.g., on the so-called spin temperature which, due to their restriction to certain parameter regimes, would only predict a homogenous quasiequilibrium state [10–12,18–23].

Model.—We model the evolution of the electron system within the framework of a Markovian Lindblad master equation. The density matrix ρ of a system consisting of N microwave-driven electrons evolves according to $\dot{\rho} = -i[H,\rho] + \mathcal{D}\rho$. The Hamiltonian H at high static magnetic field, in the rotating frame approximation, is given by

$$H = \sum_k (\omega_1 S_{kx} + \Delta_k S_{kz}) + 3\sum_{k<k'} D_{kk'} S_{kz} S_{k'z} - \sum_{k<k'} D'_{kk'} \mathbf{S}_k \cdot \mathbf{S}_{k'}. \quad (1)$$

Here ω_1 is the strength of the microwave field, Δ_k are the offsets of the electron Larmor frequencies (detunings) from the microwave carrier frequency, and $D_{kk'}$, $D'_{kk'}$ are coefficients that parameterize the strength of the anisotropic and isotropic parts of the spin-spin dipolar and exchange

 © 2017 American Physical Society

interactions [3]. Depending on the degree of order and symmetries within the sample structure, $D_{kk'}$ and $D'_{kk'}$ can either be well defined (e.g., for crystals) or random (e.g., for glasses). In amorphous materials, Δ_k are also distributed due to the anisotropic interaction of the electrons with the static field, leading to inhomogeneous broadening of the EPR line [3,13,24].

Dissipative processes are modeled by the dissipator $\mathcal{D}$ which describes single-spin relaxation and takes the form

$$\mathcal{D}=\sum_k[\gamma_{1+}\mathcal{L}(S_{k+})+\gamma_{1-}\mathcal{L}(S_{k-})+\gamma_2\mathcal{L}(S_{kz})],$$
$$\gamma_{1\pm}=\frac{R_1}{2}(1\mp p),\quad \gamma_2=2R_2,\quad p=\tanh\frac{\hbar\omega_S}{2k_BT} \tag{2}$$

where $\mathcal{L}(X)\rho\equiv X\rho X^\dagger-\{X^\dagger X,\rho\}/2$ is the Lindblad form of a dissipation operator [25]. The dissipation rates depend on the longitudinal (R_1) and transversal (R_2) relaxation rates of the electron spins as well as the thermal polarization $p\in[0,1]$, which depends on the average electron Larmor frequency ω_S and the temperature T. Note that throughout this Letter many observables will be expressed through p and thereby acquire their temperature dependence. For typical experimental conditions (W band, $\omega_S\sim 100$ GHz, sample temperature between $T\sim 0$ K and $T\sim 100$ K) p is in the region of 1–0.01.

Mean field in the absence of disorder.—In order to obtain a basic understanding of the phase structure of the driven electron system, let us first disregard any dispersion in the frequency offsets and interactions, by setting $\Delta_k=\Delta$ and $D_{kk'}=D/(N-1)$. In the nondisordered case, the last term of Eq. (1) commutes with the rest of the Hamiltonian and does not influence the bulk polarization dynamics. Therefore, we can neglect it, leading to the mean-field Hamiltonian

$$\bar{H}=\sum_k(\omega_1S_{kx}+\Delta S_{kz})+\frac{3D}{N-1}\sum_{k<k'}S_{kz}S_{k'z}. \tag{3}$$

We now compute the stationary average bulk polarization $p_z=-2\sum\mathrm{Tr}(S_{kz}\rho_{\mathrm{ss}})/N$, which serves as an order parameter for classifying the steady state ρ_{ss} and coincides (due to the system homogeneity) with the steady-state polarization of the individual spins. To obtain the mean-field equation, we consider the projection $H_k=\omega_1S_{kx}+\bar{\Delta}_kS_{kz}$ of $\bar{H}$ onto the subspace of an arbitrary spin k. Here $\bar{\Delta}_k=\Delta+[3D/(N-1)]\sum_{k'\neq k}S_{k'z}$ is the effective energy shift or offset term experienced by the spin that accounts for the frequency offset and interactions with other spins $k'\neq k$, which introduces collective effects. This effective (collective) energy shift takes discrete values

$$\bar{\Delta}_k\in\delta(q)=\Delta+\frac{3D}{N-1}\left(q-\frac{N-1}{2}\right) \tag{4}$$

where $q=0,\ldots,N-1$ is the number of spins $k'\neq k$ in the up state. For each value q, the steady-state polarization $p'_z(q)$ is given by the single-spin formula [see Supplemental Material (SM) [26]]

$$p'_z(q)=p\left(1-\frac{\eta\omega_1^2}{\delta_0^2+\delta^2(q)}\right), \tag{5}$$

where $\delta_0=\sqrt{R_2^2+\eta\omega_1^2}$ and $\eta=R_2/R_1$ is the ratio of the electron spin relaxation rates. Averaging Eq. (5) over all values of q (thus taking into account all possible orientations of the surrounding spins) finally yields the equation for the relative steady-state polarization $\bar{p}_z=p_z/p$,

$$\bar{p}_z=f(\Delta,D,\bar{p}_z)\equiv\sum_{q=0}^{N-1}P(q,p\bar{p}_z)p'_z(q)/p. \tag{6}$$

Here $P(q,p_z)=(N-1/q)\{[(1-p_z)^q(1+p_z)^{N-1-q}]/2^{N-1}\}$ is the probability of having q up spins and $N-q-1$ down spins. Since the right-hand side depends on $\bar{p}_z$, Eq. (6) should be regarded as a self-consistency condition. Note also that Eq. (6) depends on Δ, D, and temperature (via the thermal polarization p).

Low- and high-temperature regime.—The relative polarization is bounded ($|\bar{p}_z|\leq 1$); thus, $f(\bar{p}_z)$ defines a continuous map of the unit interval $\bar{p}_z\in[0,1]$ to itself. Therefore, by virtue of the Brouwer fixed-point theorem [30], Eq. (6) always has at least one solution. We find that the solution is unique for small values of p corresponding to high temperatures and small numbers of spins N (see SM [26]).

For small values of N we can compare the results of the mean-field treatment to the exact solution of the quantum master equation given by the dissipator (2) and Hamiltonian (3). To this end we show in Fig. 1(a) the steady-state polarization spectrum, i.e., the dependence of the bulk polarization $\bar{p}_z$ on the average microwave offset Δ, for three typical sets of parameters for $N=4$. Generally a good agreement is obtained. The observed spectra have N Lorentzian peaks occurring at $\Delta=3D[1/2-q/(N-1)]$, $q=0,1,\ldots,N-1$, with a half-width of δ_0. The center $\Delta=0$ of the spectrum corresponds to $q\sim q_0\equiv(N-1)/2$. The mean of the binomial distribution $P(q,p\bar{p}_z)$ where the maximal saturation is given by $\bar{q}=(N-1)(1-p\bar{p}_z)/2$. Here $\bar{q}$ is close to q_0 for small p and tends to shift from q_0 with increasing p. Hence, the intensities of the peaks are symmetric with respect to the center of the spectrum at high temperatures ($p\sim 0$) and undergo a shift from the center at low temperatures ($p\sim 1$), with the relation between p and the temperature defined through Eq. (2).

Multistability and phase transitions.—The situation qualitatively changes when entering the regime of low temperatures, i.e., large thermal polarization $p\sim 1$, and high numbers of spins $N\gg 1$. In this case (see SM [26]) Eq. (6)

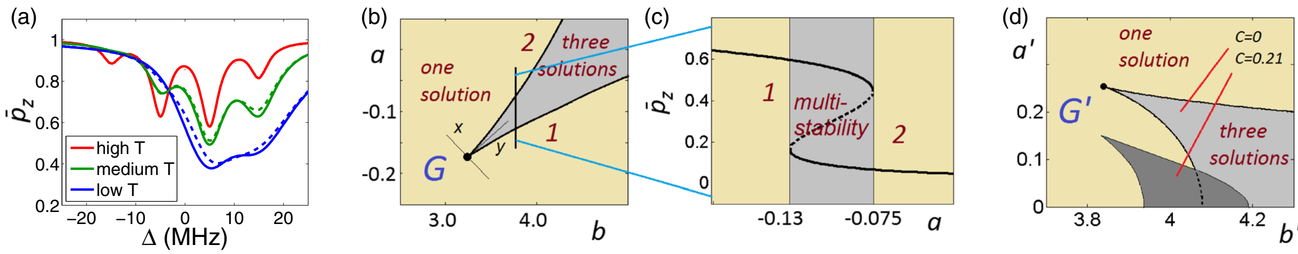

FIG. 1. (a) Steady-state polarization spectra $\bar{p}_z(\Delta)$ obtained by the mean-field formula (6) (solid lines) and the numerically exact solution (dashed lines) for $N = 4$, $D = 10$ MHz, $R_2 = 10^6\ \mathrm{s}^{-1}$, and different temperature and microwave parameters: $p = 0.11$, $\omega_1 = 75$ kHz, $R_1 = 10^3\ \mathrm{s}^{-1}$ (red); $p = 0.55$, $\omega_1 = 12$ kHz, $R_1 = 10\ \mathrm{s}^{-1}$ (green); $p = 0.99$, $\omega_1 = 7$ kHz, $R_1 = 1\ \mathrm{s}^{-1}$ (blue). (b) Phase diagram obtained from Eq. (6) in the (a, b) plane. The diagram features regions of unique (brown) and multiple (gray) solutions and displays a (cusp) critical point G at $p = 0.99$, $\omega_1 = R_2 = 10^5$, and $R_1 = 1\ \mathrm{s}^{-1}$ (for $N = 150$ electrons). (c) Structure of the solutions along the cut $b = 3.75$ ($D = 6.3$ MHz) through the region with a multistable region featuring three solutions. (d) Phase diagram obtained from Eq. (7) in the (a', b') plane featuring regions of unique and multiple solutions similar to that in panel (b) and a critical point G' belonging to the same universality class as G (see text for details). The dark gray region illustrates the impact of disorder in the frequency offsets Δ_k (inhomogeneous broadening) on the multistability region. The strength of the inhomogeneous broadening is parameterized by c (see SM [26] for details).

can feature more than one solution. In Fig. 1(b) we show the phase diagram given by the number of solutions of Eq. (6) in terms of the scaled offset and interaction parameters $a = \Delta/\omega_1\sqrt{\eta}$, $b = 3D/\omega_1\sqrt{\eta}$. Figure 1(b) features a multistability region where three solutions coexist (gray) separated from the regions with a unique solution (brown) by two spinodal lines. The point at which the coexistence region vanishes defines a critical point G, the nature of which can be characterized by analyzing the scaling behavior of the polarization $\bar{p}_z$ in two directions that are singled out: one is given by the curve that is tangent to both spinodal lines [see Fig. 1(b)], where we find $|\bar{p}_z - \bar{p}_{\mathrm{crit}}| \sim y^{1/2}$, with $\bar{p}_{\mathrm{crit}}$ being the value of $\bar{p}_z$ at the critical point. Along the perpendicular direction we find $|\bar{p}_z - \bar{p}_{\mathrm{crit}}| \sim x^{1/3}$ [27]. These are the mean-field scalings of the Ising universality class [14,31]. In other words, the direction y can be thought of as being analogous to temperature in the Ising model, where below the critical temperature, i.e., upon crossing the critical point, two ferromagnetic states emerge. Within this analogy the perpendicular direction x can be regarded as magnetic field (see SM [26] for further details). Similar phase diagrams have recently been found in other contexts, e.g., for open driven gases of strongly interacting Rydberg atoms [14,32–34], laser-polarized quantum systems [35], or certain classes of dissipative Ising models [16,17,29,36].

The behavior of the steady-state polarization $\bar{p}_z$ upon crossing the multistable region is shown in Fig. 1(c). Solutions with small $\bar{p}_z \sim 0$ correspond to nonthermal quasisaturated equilibrium states. States with large values $\bar{p}_z \sim 1$ are unsaturated quasithermal equilibria. On crossing the spinodal curve 1 from large negative values of a, the unique stable quasithermal steady state continues to exist but two other steady-state solutions appear: a stable quasisaturated one and an unstable intermediate one, as shown in Fig. 1(c). Conversely, on crossing curve 2 towards large negative values of a, the unique stable quasithermal steady state continues to exist but two other steady-state emerge, a stable and an unstable one. Note that the occurrence of multiple steady-state solutions is an artifact of the mean-field approximation which can be interpreted as the emergence of metastable states [16] near first-order phase transitions. Experimentally those may manifest through hysteretic behavior, as recently shown in [32–34]. We will return to this point further below.

Disordered spin-spin interactions and augmented mean field.—The results so far indicate possible phase transitions in the polarization of the electron system controlled by the frequency offset Δ and the average interaction strength D. However, typical sample materials are not single crystals and electrons are arranged randomly, such that the average interaction experienced by an electron is close to zero [13]. In order to take this into account we need an augmented mean-field description which accounts for a distribution in the coupling strengths.

Note that when the disorder in either the offsets Δ_k or the interactions $D_{kk'}$ is large enough, unitary dynamics with Hamiltonian (1) is expected to undergo many-body localization (MBL) [37]. In this case spatial fluctuations in the long-time state can be significant and determined by the disorder and the initial state, which raises the question of the appropriateness of mean field. However, in the presence of dissipation, cf. Eq. (2), the nonergodic MBL phase is unstable and the stationary state becomes delocalized [38–40]. This suggests that the mean-field analysis is still appropriate as long as only static (long-time properties) are investigated. The approach to stationarity may nevertheless display a transient nonergodic effect. For other possible connections between MBL and DNP see [23,41].

For the sake of simplicity we assume that the interactions D follow a Gaussian distribution, $\chi(D) = \exp(-D^2/D_0^2)/(\sqrt{\pi}D_0)$, with zero mean and standard deviation D_0. The offset frequency Δ may also be disordered (e.g., from the g

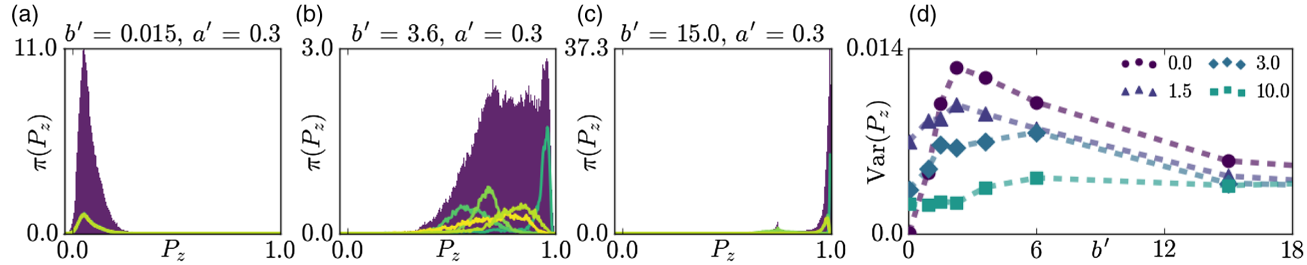

FIG. 2. Numerical simulations and fluctuations. All results in this figure are produced for parameters $\omega_1 = 10^5$ Hz, $R_1 = 1\ \mathrm{s}^{-1}$, $R_2 = 10^5\ \mathrm{s}^{-1}$, $p = 0.99$, and $N = 8$, and averaged over 10 disorder realizations. (a)–(c) Discrete approximations of the probability density (dark shaded area) for the observable P_z for three sets of parameters, such that $\int \pi(P_z) dP_z = 1$ over the range shown. The light-colored curves represent the densities for some individual disorders, divided by the number of disorder realizations considered so that their addition (rather than their average) would equal the full probability density. This is done to better represent the contribution each disorder realization makes to the distribution. Panel (b) shows a strongly broadened distribution signaling enhanced fluctuations. This is consistent with the presence of metastable states that are expected from the mean-field analysis. (d) The variance of the time integrated observable P_z for varying b', with the fixed a' value indicated by the legend in the top right.

anisotropy and hyperfine interactions with nuclei [3,24]), but we neglect that effect for now. With disorder Eq. (6) generalizes to

$$\bar{p}_z = \int_{-\infty}^{+\infty} f_0(\Delta, D, \bar{p}_z)\chi(D) dD. \qquad (7)$$

To obtain this expression we averaged over $\chi(D)$ and additionally exploited the fact that in the thermodynamic limit ($N \gg 1$) the function f on the right-hand side of Eq. (6) coincides with the function $f_0 = p_z'(\bar{q})/p$, where $\bar{q} = (N-1)(1 - p\bar{p}_z)/2$ is the mean of the binomial distribution $P(q, p\bar{p}_z)$. This gives $f_0 = 1 - \eta\omega_1^2/(\delta_0^2 + \delta^2)$ with $\delta = \Delta - 3Dp\bar{p}_z/2$ (see SM [26]). The mean-field phase diagram resulting from Eq. (7) is displayed in Fig. 1(d) as a function of the dimensionless parameters $a' = \Delta_0/\omega_1\sqrt{\eta}$ (Δ_0 is the average offset, equal to Δ in the case considered here) and $b' = 3pD_0/2\omega_1\sqrt{\eta}$. We assume that the strength of the microwave field is large, $\omega_1^2\eta \gg R_2^2$, meaning that the electron system is fully saturated in the absence of spin-spin coupling (in which case the phase transitions observed are most pronounced). The structure is similar to that of Fig. 1(b). We observe regions with one and three solutions as well as spinodal lines forming a cusp at a critical point G'. The scaling properties at this critical point are again those of mean-field Ising universality. Although equal to the nondisordered case, the important point is that the underlying mechanism is different. In the presence of disorder the phase transition is controlled by the width of the distribution of the disorder strengths ($D_0 \propto b'$) rather than the average interaction strength, which is in fact zero.

Fluctuations and numerical simulations.—The mean-field treatment above is of course not exact. Whether the predicted qualitative phase structure survives away from mean field depends on the effect of fluctuations [29,36]. As shown in [15–17], phase coexistence at the mean-field level can be an indication—away from the thermodynamic limit [29] of the existence of long-lived metastable (rather than stationary) phases. These competing phases come with an intermittent dynamics of slow switching between them and a significantly longer relaxation time. While the value of the polarization will fluctuate over time within these phases, it will take a distinct average value in each phase. We now show that this is indeed the case by investigating the numerically exact polarization dynamics for a small system, Eqs. (1) and (2), by means of quantum jump Monte Carlo simulations [28]. In particular we monitor the time dependence of the polarization $p_z(t) = -(2/N)\sum_k \mathrm{Tr}[S_{kz}\rho(t)]$ for a variety of values of a' and b'. For the set of parameters we consider, multiple disorder realizations of the dipolar coupling $\{D_{kk'}\}$, with $D'_{kk'} = D_{kk'}$, are taken. These are independent and identically distributed, sampled from a Gaussian distribution with variance defined by b' (see SM [26] for details).

Fluctuations due to metastability can be quantified by the probability distribution of the time-integrated polarization, $P_z = (1/t)\int_0^t p_z(t')dt'$. As t is increased in systems without metastability we expect a contracting distribution with a single, approximately Gaussian, peak around the stationary state value. In the presence of metastability we instead expect a broadened, non-Gaussian distribution. In particular, for t on the order of metastable phase lifetimes one expects multiple peaks located near the average values of the different metastable phases. While we lack the distinct metastable phases due to small sizes and disorder, for t on the order of relaxation time, Figs. 2(a)–2(c) show an intermediate regime in which the disorder-averaged distribution is strongly broadened and non-Gaussian. In Fig. 2(d) we plot the variance as a function of b' for several values of a', cf. Fig. 1(d). We see a peak at intermediate values of b' for all curves, which is consistent with the expectation of a phase transition in the thermodynamic limit.

Conclusions.—Our results demonstrate that cooperative behavior in strongly interacting ensembles of microwave-driven electrons—a situation of relevance to DNP in

NMR—can give rise to a nontrivial phase structure in the stationary state of these systems. While the calculated phase diagram is mean field in origin, our simulations show that—even for finite systems—dynamics will be correlated and intermittent, related to the coexistence of metastable states. In the future, further insights could be gained by using the augmented mean-field methods for open quantum systems [42]. The experimental demonstration of the predicted phenomena would ideally require a paramagnetic sample with minimal inhomogeneous broadening, kept at cryogenic temperatures and high magnetic field.

The authors thank B. Olmos and J. A. Needham for useful discussions. The research leading to these results has received funding from the European Research Council under the European Union's Seventh Framework Programme (FP7/2007–2013)/ERC Grant No. 335266 (ESCQUMA) and the EPSRC Grant No. EP/N03404X/1. We are also grateful for access to the University of Nottingham High Performance Computing Facility.

[1] E. Zavoisky, J. Phys. USSR **9**, 211 (1945).
[2] G. Lancaster, J. Mater. Sci. **2**, 489 (1967).
[3] A. Schweiger and G. Jeschke, *Principles of Pulse Electron Paramagnetic Resonance* (Oxford University Press, New York, 2001).
[4] Special issue on dynamic nuclear polarization, edited by R. G. Griffin, T. F. Prisner, and C. P. Slichter [Phys. Chem. Chem. Phys. **12**, 5725 (2010)].
[5] Special issue on dynamic nuclear polarization, edited by A. V. Atsarkin and W. Köckenberger [Appl. Magn. Reson. **43**, 1 (2012)].
[6] W. T. Wenckebach, *Essentials of Dynamic Nuclear Polarisation* (Spindrift Publications, The Netherlands, 2016).
[7] A. Kessenikh, V. Luschikov, and A. Manenkov, Phys. Solid State **8**, 835 (1963).
[8] C. F. Hwang and D. A. Hill, Phys. Rev. Lett. **19**, 1011 (1967).
[9] K. N. Hu, H. H. Yu, T. M. Swager, and R. G. Griffin, J. Am. Chem. Soc. **126**, 10844 (2004).
[10] M. Borghini, Phys. Rev. Lett. **20**, 419 (1968).
[11] V. A. Atsarkin and M. I. Rodak, Phys. Usp. **15**, 251 (1972).
[12] A. Abragam and M. Goldman, *Nuclear Magnetism: Order and Disorder* (Clarendon Press, Oxford, 1982).
[13] A. Karabanov, G. Kwiatkowski, C. U. Perotto, D. Wiśniewski, J. McMaster, I. Lesanovsky, and W. Köckenberger, Phys. Chem. Chem. Phys. **18**, 30093 (2016).
[14] M. Marcuzzi, E. Levi, S. Diehl, J. P. Garrahan, and I. Lesanovsky, Phys. Rev. Lett. **113**, 210401 (2014).
[15] M. Foss-Feig, P. Niroula, J. T. Young, M. Hafezi, A. V. Gorshkov, R. M. Wilson, and M. F. Maghrebi, Phys. Rev. A **95**, 043826 (2017).
[16] D. C. Rose, K. Macieszczak, I. Lesanovsky, and J. P. Garrahan, Phys. Rev. E **94**, 052132 (2016).
[17] C. Ates, B. Olmos, J. P. Garrahan, and I. Lesanovsky, Phys. Rev. A **85**, 043620 (2012).
[18] B. N. Provotorov, J. Exp. Theor. Phys. **14**, 1126 (1962).
[19] V. A. Atsarkin, Phys. Usp. **21**, 725 (1978).
[20] S. Jannin, A. Comment, and J. van der Klink, Appl. Magn. Reson. **43**, 59 (2012).
[21] Y. Hovav, A. Feintuch, and S. Vega, Phys. Chem. Chem. Phys. **15**, 188 (2013).
[22] S. C. Serra, A. Rosso, and F. Tedoldi, Phys. Chem. Chem. Phys. **14**, 13299 (2012).
[23] A. De Luca and A. Rosso, Phys. Rev. Lett. **115**, 080401 (2015).
[24] C. P. Poole and H. A. Farach, Bull. Magn. Reson. **1**, 162 (1979).
[25] A. Karabanov, D. Wiśniewski, I. Lesanovsky, and W. Köckenberger, Phys. Rev. Lett. **115**, 020404 (2015).
[26] See Supplemental Material at http://link.aps.org/supplemental/10.1103/PhysRevLett.119.150402 for details on the construction and phase structure analysis of the mean-field theory, both with and without disorder, along with a description of the numerical approach used to simulate the full model. These details rely on results contained in Refs. [14,16,17,27–29].
[27] V. I. Arnold, *Catastrophe Theory* (Springer Verlag, Berlin, 1984).
[28] A. J. Daley, Adv. Phys. **63**, 77 (2014).
[29] S. G. Schirmer and X. Wang, Phys. Rev. A **81**, 062306 (2010).
[30] L. E. J. Brouwer, Math. Ann. **71**, 97 (1911).
[31] N. Goldenfeld, *Lectures on Phase Transitions and the Renormalisation Group* (Addison-Wesley, Reading, MA, 1992).
[32] C. Carr, R. Ritter, C. G. Wade, C. S. Adams, and K. J. Weatherill, Phys. Rev. Lett. **111**, 113901 (2013).
[33] N. R. de Melo, C. G. Wade, N. Šibalić, J. M. Kondo, C. S. Adams, and K. J. Weatherill, Phys. Rev. A **93**, 063863 (2016).
[34] D. Weller, A. Urvoy, A. Rico, R. Löw, and H. Kübler, Phys. Rev. A **94**, 063820 (2016).
[35] A. A. Zvyagin, Phys. Rev. B **93**, 184407 (2016).
[36] H. Weimer, Phys. Rev. Lett. **114**, 040402 (2015).
[37] R. Nandkishore and D. A. Huse, Annu. Rev. Condens. Matter Phys. **6**, 15 (2015).
[38] E. Levi, M. Heyl, I. Lesanovsky, and J. P. Garrahan, Phys. Rev. Lett. **116**, 237203 (2016).
[39] M. V. Medvedyeva, T. Prosen, and M. Žnidarič, Phys. Rev. B **93**, 094205 (2016).
[40] M. H. Fischer, M. Maksymenko, and E. Altman, Phys. Rev. Lett. **116**, 160401 (2016).
[41] A. De Luca, I. R. Arias, M. Müller, and A. Rosso, Phys. Rev. B **94**, 014203 (2016).
[42] J. Jin, A. Biella, O. Viyuela, L. Mazza, J. Keeling, R. Fazio, and D. Rossini, Phys. Rev. X **6**, 031011 (2016).